Title: A Hierarchical Approach to Three-Dimensional Segmentation of LiDAR Data at Single-Tree Level in a Multilayered Forest

This paper appears in: IEEE Transactions on Geoscience and Remote Sensing

Date of Publication: 05/04/2016

Author(s): Claudia Paris, Davide, Valduga, Lorenzo Bruzzone

Volume:PP, Issue: 99

Page(s): 1 - 14

DOI: 10.1109/TGRS.2016.2538203

A Hierarchical Approach to Three-Dimensional Segmentation of LiDAR Data at Single Tree Level in Multi-Layered Forest

Claudia Paris, *Student Member, IEEE*, Davide Valduga, Lorenzo Bruzzone, *Fellow, IEEE*

***Abstract*—Small-footprint high-density LiDAR data provide information on both the dominant and the subdominant layers of the forest. However, tree detection is usually carried out in the Canopy Height Model (CHM) image domain, where not all the dominant trees are distinguishable and the understory vegetation is not visible. To address these issues, we propose a novel method that integrates the analysis of the CHM with that of the Point Cloud Space (PCS) to: i) improve the accuracy in the detection and delineation of the dominant trees, and ii) identify and delineate the subdominant trees. By means of a derivative analysis of the horizontal profile of the forest, the method detects the missed crowns and delineates the crown boundaries directly in the PCS. Then, for each segmented crown, the vertical profile is analyzed to identify the presence of subcanopies and extract them. The proposed method does not require any prior knowledge on the stand properties (e.g., crown size, forest density). Experimental results obtained on two LiDAR datasets characterized by different laser point density show that the proposed method always improved the detection rate compared to other state-of-the-art techniques. It correctly detected 97% and 92% of the dominant trees measured in situ in high- and low-density LiDAR data, respectively. Moreover, it automatically identified 77% of the subdominant trees manually extracted by an expert operator in the high-density LiDAR data.**

***Index Terms*—Forestry, individual tree crown detection, Light Detection and Ranging (LiDAR), remote sensing, segmentation, tree crown delineation.**

I. Introduction

THE accurate characterization of the 3-D structure of the forest is becoming essential for modern forest inventories. One of the most effective remote sensing technology used for the estimation of forest parameters is based on airborne Light Detection and Ranging (LiDAR) systems. Due to the capability of the laser scanner to measure the vertical structure of the forest, it is possible to accurately retrieve tree variables. In particular, small-footprint high-resolution LiDAR data provide detailed information on the dominant layer of the forest and are able to collect measures on the subcanopy layers. In this framework, the detection and the segmentation of single tree crowns represent a fundamental step to accurately estimate individual tree structural attributes of both the dominant and the subdominant trees.

Several methods to extract the single tree crowns from LiDAR data have been developed. Most of them detect the trees in the Canopy Height Model (CHM), i.e., the rasterized image derived from the normalized LiDAR point cloud [1], [2], [3], [4], [5]. The treetops are usually identified with the peaks in the CHM detected with a Local Maxima Filtering Algorithm. However, the detection rate in the raster-based methods is strongly affected by the spatial resolution of the CHM and the smoothing factor, which is necessary to reduce the noise and emphasize the crown borders. Moreover, in mixed forest characterized by variable crown sizes it is not possible to find an optimal smoothing factor [6]. Furthermore, there are no reliable rules to select the spatial resolution of the CHM, which is related to the application type and the properties of the dataset [7]. To address this issue, in [8] the authors develop a strategy to identify the best CHM resolution at plot level by modelling the spatial stem distribution of the sample plot. By testing a set of candidate pixel sizes, the best spatial resolution is selected as the one that allows the detection of a number of local maxima equals to the predicted number of stems. However, the method relies on the assumptions that all the trees are visible in the image and that the number of trees can be accurately estimated.

After the detection phase, the crowns are typically segmented around the treetop considering region growing methods [4], [9], [10], watershed or pouring algorithms [11], [12], [8], [6], [13], [14], or techniques based on template matching [15], [16], [17]. However, when the segmentation is performed in the CHM the result is affected by the artefacts introduced in the rasterization process (e.g., interpolation). In heterogeneous forests combinations of tree groups can be segmented in one single crown due to smoothing, thus degrading the accuracy of the inventory estimates [18]. To solve this problem, in [9] the region growing segmentation results are constrained by imposing rules on the shape of the crowns, whereas in [14] the watershed algorithm is driven by a prior estimation of the canopy size. However, by comparing the segmentation results obtained on both the CHM and the LiDAR point cloud space, one can observe that the highest accuracy is obtained in the point cloud domain [19].

For the reasons mentioned earlier, some methods address the detection in the CHM and the segmentation in the LiDAR point cloud, where the crowns are usually extracted by using a k-mean clustering algorithm [20], [21], [22]. In [20] the authors initialize the clusters by using both a set of randomly selected seeds and a set of local maxima extracted in the CHM. Moreover, they investigate the possibility of scaling down the height value instead of using the original one, to minimize the intracluster variance and fit the conical shape of the crown. As expected, the highest accuracies are obtained by initializing the algorithm with the detected treetops and rescaling the height

value. Indeed, as discussed in [21], the Euclidean metric used to drive the clustering algorithm tends to generate ball-shaped clusters of LiDAR points. However, the main drawback of the detection algorithms applied to the image domain is that they are not able to extract the understory vegetation [23]. It is worth noting that an accurate detection of the subcanopy layers represents an important task for fire behaviour models [24] as well as forest management and planning.

To solve this problem, several papers present methods that perform the segmentation of the dominant trees in the CHM and then analyze the LiDAR point cloud to detect the understory vegetation layer. In [25] the authors present a 3D segmentation method applied to full-waveform LiDAR data. First, a watershed segmentation algorithm is employed to delineate the dominant tree crowns. Second, the segmented regions are refined by detecting the tree stems. Finally, the small trees are detected using the normalized cut segmentation approach presented in [26]. Although this technique is able to obtain an high detection rate for small trees, many false trees are identified. Moreover, the detection of the understory vegetation strongly depends on several parameters. The same problem is encountered in [27], where an ellipsoidal k-mean clustering algorithm is directly applied to the LiDAR point cloud after having detected the dominant tree crowns in the CHM. For detecting the subdominant trees, the cluster centers are placed at regular horizontal distance, while the height is set as half of the mean height of the dominant trees. The segmentation result is finally refined by fitting an ellipsoid surface. However, many subdominant crowns delineated do not correspond to any field-measured tree. In contrast, in [28] the authors perform the detection of the subdominant trees without tuning any parameters or thresholds. For each dominant crown the height frequency distribution is interpolated with a polynomial function. By analyzing the behaviour of the interpolated curve it is possible to determine the presence of understory vegetation. A similar analysis is performed in [29], where the height distribution probability function of the LiDAR points is analyzed to split the data into two canopy layers. However, this approach relies on the assumption that the forest structure is characterized by two layers which are separable by a plane. In [30], the vertical profile of the dominant tree crowns delineated in the CHM by means of a watershed algorithm is analyzed to detect understory vegetation in multi-layered forest. The identification of the different layers of the forest has been also addressed by applying a statistical analysis of the LiDAR point cloud [31], [32], [33], [34].

From this brief analysis of the literature one can notice that an accurate detection and delineation of the dominant and the subdominant trees presents critical issues especially when dealing with dense forest scenarios [35], [36]. The majority of the methods require prior knowledge on the considered forest area and unrealistic homogeneity assumptions on the average crown size and forest density. To solve this problem, several papers developed crown size adaptive methods [6], [37], [38], [39]. However, many of them exploit only the image domain, which is affected by the interpolation of the LiDAR data. In contrast, the methods that detect the trees in the 3D point cloud have the problems of choosing the right scale [40] and of dealing with the irregular sampling of the canopies by the laser pulses [41]. Few hybrid approaches combine the image and point cloud domains [20], [22], [30]. However, none of them takes advantage from the joint use of the two domains to improve the tree detection obtained by using each single domain. In this framework, we propose a hierarchical 3D segmentation approach to detect and delineate both dominant and subdominant tree crowns by using high-density LiDAR data. Unlike the methods presented in the literature, the proposed approach does not require any prior knowledge on the crown size and forest density, but relies on the geometrical structure of the forest and the properties of the LiDAR data. Thus, it can be successfully applied to large forest areas characterized by heterogeneous 3D crown structures. In greater detail, the proposed method: i) exploits both the image and the point cloud domains to detect the dominant trees, ii) delineates the dominant tree crown directly in the PCS by means of a derivative analysis of the horizontal structure of the forest, iii) identifies the subdominant trees by analyzing the 3D vertical profile of the dominant trees in different angular sectors, and iv) extracts the understory vegetation.

The main novelties of the proposed approach are: i) the use of the LiDAR point cloud to detect the trees missed in the CHM image domain, ii) the use of the LiDAR point cloud to identify the position of the subdominant trees located in different sides of the dominant tree crowns by means of an angular analysis, iii) the crown delineation method for both dominant and subdominant trees based on the derivative analysis of the horizontal profile of the trees in the LiDAR point cloud. The effectiveness of the proposed method is demonstrated in experiments carried out in a complex dense forest scenario located in the Southern Alps of the Trentino region (Italy) by using high-density LiDAR data (up to 50 pts/m^2) and low-density LiDAR data (up to 8 pts/m^2).

The paper is organized as follows: Section II presents the architecture of the proposed method and describes in detail the steps of the presented technique. Section III illustrates the dataset, and Section IV reports an analysis of the parameters required by the proposed method and describes the experimental setup. Section V presents and discusses the experimental results. Finally, Section VI draws the conclusions of the work. The mathematical notation used in the paper is listed in the appendix.

II. Proposed Hierarchical 3D Segmentation Approach

The proposed method aims to accurately extract all the trees detectable in the LiDAR data. To decompose the segmentation process and thus to facilitate the tree detection, we exploit a hierarchical approach which concentrates sequentially on the dominant and on the subdominant layers of the forest. Fig. 1 shows the block scheme of the proposed method. It is worth noting that the PCS represents the normalized LiDAR point cloud obtained after the subtraction of the digital terrain model.

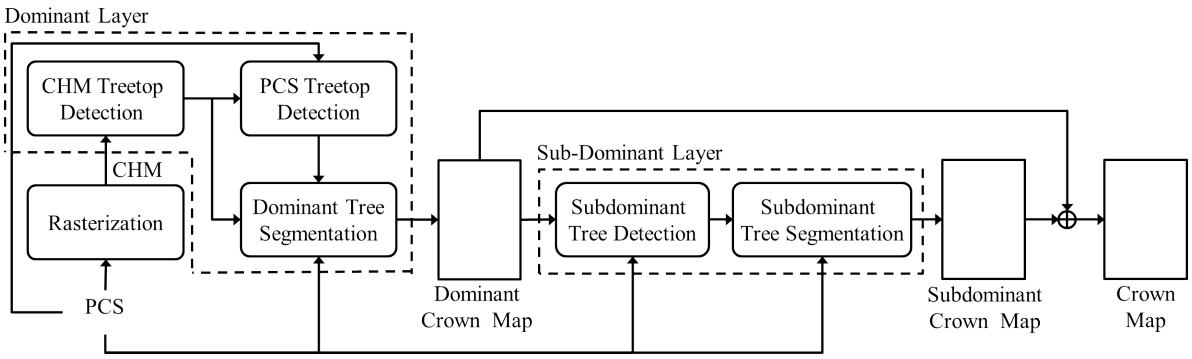

Fig. 1. Architecture of the proposed hierarchical approach to 3D segmentation of the dominant and the subdominant crowns.

A. Detection of Dominant Trees

In this step we aim to identify the dominant trees present in the scene by exploiting both the CHM and the PCS for taking advantage from the complementarity of the two domains. While in the CHM it is possible to detect the majority of the trees present in the scene with a low computational load, the analysis of the PCS allows us to identify the missed trees. First, a coarse analysis is performed in the image domain by applying a level set method [42]. Then, the analysis is refined in the PCS to detect close neighbouring treetops that may not appear clearly separated in the CHM but are visible in the point cloud.

Let $\mathcal{P} = \{\mathbf{p}_i\}_{i=1}^{A}$ be the set of LiDAR points of the PCS and let $\mathcal{T}_{\text{CHM}} = \{\mathbf{t}_k\}_{k=1}^{M}$ be the set of treetops detected in the CHM. Note that $\mathbf{p}_i$ and $\mathbf{t}_k$ are three-element row vectors defined by the x, y, z coordinates, i.e., $\mathbf{p}_i = (x_i, y_i, z_i)$ and $\mathbf{t}_k = (x_k^t, y_k^t, z_k^t)$. To identify possible missed crowns, we analyze the forest area around each detected treetop directly in the PCS. Let us define $\mathcal{P}_k$ as the set of LiDAR points extracted around the treetop $\mathbf{t}_k$ within a given search radius R, which is large enough to represent the surrounding crowns (e.g., three times the crown radius). The detection of the neighbouring treetops in different directions is performed by means of an angular analysis which partitions $\mathcal{P}_k$ into N angular sectors. Let Θ_j be the angular partition between the adjacent angles $\theta_j = 2\pi j/N$ and $\theta_{j+1} = 2\pi(j+1)/N$, with $j \in [0, N\text{-}1]$ (see Fig. 2a and Fig. 2b). The set of LiDAR points belonging to the angular sector $\mathcal{P}_{k,\Theta_j}$ is defined as:

$$\mathcal{P}_{k,\Theta_j} = \left\{ \mathbf{p}_i \in \mathcal{P}_k \middle| \arctan\left(\frac{x_i - x_k^t}{y_i - y_k^t}\right) \in [\theta_j, \theta_{j+1}) \right\} \quad (1)$$

To detect the treetop of the neighbouring trees, we model the angular sector with a 1D discrete signal $S_{k,\Theta_j}(\rho)$, composed by the coordinates z_i of the LiDAR points $\mathbf{p}_i \in \mathcal{P}_{k,\Theta_j}$ and depending on their distances from the treetop, i.e., $\rho_i = \sqrt{(x_i - x_k^t)^2 + (y_i - y_k^t)^2}$. To this end, we first apply a circular projection to the points $\mathbf{p}_i \in \mathcal{P}_{k,\Theta_j}$ onto the ρz plane centered in the treetop coordinates (x_k^t, y_k^t). Let us define $\Pi_c : (x, y, z) \mapsto (\rho, z)$ as the circular projection that allows us to map the points from the 3D space $\mathbf{R}^3$ onto the 2D space $\mathbf{R}^2$ (see Fig. 2c). Then, because we are interested in the crown surface, we keep the set of highest points belonging to the first return. Accordingly, we quantize the distance of the points from the treetop $\rho_i \in [0, R]$ into F intervals $\xi = R/F$ and select the maximum height value in each ξ (see Fig. 2d). Note that, the quantization step should be tuned considering the characteristics of the LiDAR data (i.e., footprint, point density), to guarantee that, in each interval ξ, the highest LiDAR point represents the crown surface. A similar angular analysis has been performed in [43], where the authors aim at refining a manual segmentation of tree crowns based on field measurements, by removing those sectors including LiDAR points of the neighbouring trees. In particular, they represent the angular sector considering the mean height values in each interval ξ =0.5 m. Then, by evaluating the trend of the sector profile, they determine possible oversegmentation. In contrast, we consider the maximum height value per interval to represent the shape of the crown and we aim to detect the position of the closest treetop.

A Gaussian filtering is then applied to $S_{k,\Theta_j}(\rho)$ in order to trim upper branches and thus avoid false local maxima. Unlike filtering applied in the image domain, we do not lose any detail while still smoothing the conical shape of the crown. Finally, for each 1D signal $S_{k,\Theta_j}(\rho)$ we compute the discrete derivative $S'_{k,\Theta_j}(\rho)$ to detect the closest local height maximum, i.e,:

$$M_{k,\Theta_j} = S_{k,\Theta_j}(\rho_0), \text{ with } \rho_0 = \underset{\rho}{\text{argmax}}\left\{ S_{k,\Theta_j}(\rho) \right\} \quad (2)$$

To avoid false treetops detection, a local maximum is considered a treetop when it is detected from at least two different tree apexes identified in the CHM. This is based on the reasonable assumption that a missed apex is surrounded by more than one tree. Since we are dealing with dense forest scenarios, this cross-check allows us to avoid false local maxima without losing possible treetops. The new set of candidate treetops $\mathcal{T}_{\text{PCS}}$ is then compared with the set of treetops $\mathcal{T}_{\text{CHM}}$ to remove the redundancy. At the end of this step, we obtain the whole set of tree apexes $\mathcal{T} = \{\mathbf{t}_k\}_{k=1}^{W}$.

Note that the hybrid approaches presented in the literature typically refine the segmentation results obtained in the CHM by detecting the tree stems [25] or by fitting parametric models to the segmented point clouds [44]. However, tree stems are not always visible (particularly in dense forest scenario). Moreover, to obtain accurate detection results it is necessary to properly tune the model parameters. In contrast, the proposed method jointly uses the images and the point cloud domains

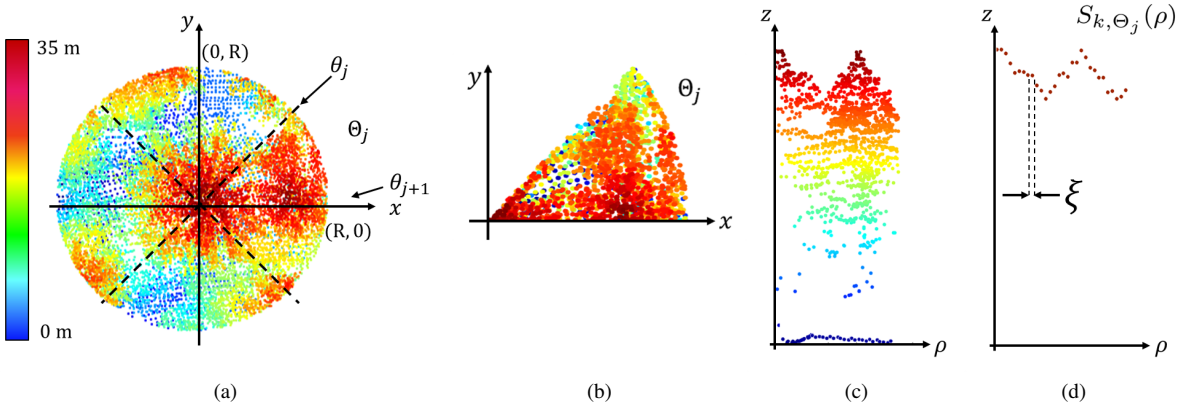

(a) (b) (c) (d)

Fig. 2. Example of angular analysis: (a) top view of the LiDAR point cloud $\mathcal{P}_k$ divided into N angular sectors, with N=8, (b) top view of the LiDAR points belonging to the angular sector Θ_j, (c) side view of the LiDAR points belonging to the angular sector Θ_j after the circular projection onto the ρz plane, (d) side view of the one-dimensional discrete signal $S_{k,\Theta_j}(\rho)$ that approximates the shape of the crown in the sector Θ_j.

to improve the detection of the trees by relying only on the geometrical structure of the crown. Furthermore, the proposed analysis of the PCS is not computationally demanding and thus can be easily applied to large forest areas.

B. Crown Delineation of Dominant Trees

To address the drawbacks of the segmentation methods applied to the CHM, clustering techniques are usually applied to the PCS to delineate the crowns [21], [20]. However, the bottleneck of these techniques is the computational burden since they need to process the entire point cloud. Moreover, they do not consider the physical properties of the shape of the crown to perform the segmentation. In contrast, we aim to exploit the geometrical structure of the crowns to segment each single tree. By considering an angular analysis we are able to adapt the segmentation to the different portions of the crown by analyzing each angular partition separately. Moreover, by focusing the attention on the set of LiDAR points $\mathcal{P}_k$ extracted around the treetop $\mathbf{t}_k \in \mathcal{T}$ within a radius R we strongly reduce the computational load. As in the previous case, by modelling $\mathcal{P}_{k,\Theta_j}$ with the discrete 1D signal $S_{k,\Theta_j}(\rho)$, the position of the edge E_{k,Θ_j} can be associated to the first local minimum detected computing the discrete derivative $S'_{k,\Theta_j}(\rho)$, i.e.,

$$E_{k,\Theta_j} = S_{k,\Theta_j}(\rho_0), \text{ with } \rho_0 = \underset{\rho}{\operatorname{argmin}}\{S_{k,\Theta_j}(\rho)\} \quad (3)$$

By analyzing the distance ρ_i of the LiDAR points $\mathbf{p}_i \in \mathcal{P}_{k,\Theta_j}$ from the treetop $\mathbf{t}_k$, we can identify the points belonging to the crown $\mathcal{C}_k$ that are those having $\rho_i \leq E_{k,\Theta_j}$. At the end of this step the edge positions E_{k,Θ_j} with $j \in [0, N\text{-}1]$ within the angular sectors have been identified. Therefore, we can delineate the crowns directly in the PCS thus generating the set of segmented crowns $\{\mathcal{C}_k\}_{k=1}^{W}$, where for each detected treetop $\mathbf{t}_k \in \mathcal{T}$ we associate the set of LiDAR points $\mathcal{C}_k = \{\mathbf{p}_1, \mathbf{p}_2, .., \mathbf{p}_B\}$ belonging to the crown. Note that the size of the angular sectors can be the same of the one used for the detection of the treetop. However, to better delineate the crown contours it is possible to increase the number of angular sectors as long as there is a sufficient number of LiDAR points in each Θ_j to represent the shape of the crown. Finally, we check the set of trees detected by means of the derivative analysis to assess that those segmented point clouds have a minimum number of LiDAR points. Indeed, in the case upper branches might appear as local maxima in the derivative analysis, the crowns delineated around them can be easily removed because they result in few LiDAR points. Note that, unlike the state-of-the-art methods, the proposed approach can perform the segmentation of each crown separately and in parallel thus strongly reducing the computational effort.

C. Detection of subdominant Trees

In this paper we refer to subdominant trees considering all the trees covered by upper canopies. Therefore, we are not assuming that the forest is characterized by two layers of trees, but we can address the multilayered forest case. To automatically detect the understory vegetation, we first split each segmented crown $\mathcal{C}_k$ into L angular sectors (see Fig. 3a and Fig. 3b), large enough to allow the detection of the subdominant trees. Thus, the number of angular sectors could be different from the number of sectors employed to perform the dominant tree crowns segmentation, i.e., $L \leq N$. Second, we analyze the vertical profile of each sector to detect both the presence and the height of the subdominant trees. Indeed, if there is a subcanopy, it is reasonable to assume the presence of a hump in the bottom part of the vertical profile of the angular sector of the crown (see Fig. 3c), otherwise not visible (see Fig. 3f). Accordingly, we model the angular sector $\mathcal{C}_{k,\Theta_j}$ with the 1D vertical discrete signal $V_{k,\Theta_j}(z)$, composed of the distances from the treetop ρ_i of the LiDAR points $\mathbf{p}_i \in \mathcal{C}_{k,\Theta_j}$ and depending on the height coordinates z_i. To this end, we first apply the circular projection Π_c to the LiDAR points $\mathbf{p}_i \in \mathcal{C}_{k,\Theta_j}$. Let H_{k,Θ_j} be the maximum height value of the set of points $\mathcal{C}_{k,\Theta_j}$. Second, we quantize the height values $z_i \in [0, H_{k,\Theta_j}]$ into D steps $\delta = H_{k,\Theta_j}/D$ and select in each δ the LiDAR point having maximum distance ρ_i from the treetop $\mathbf{t}_k$ (see Fig. 3d and 3g). Finally, a Gaussian filtering is applied

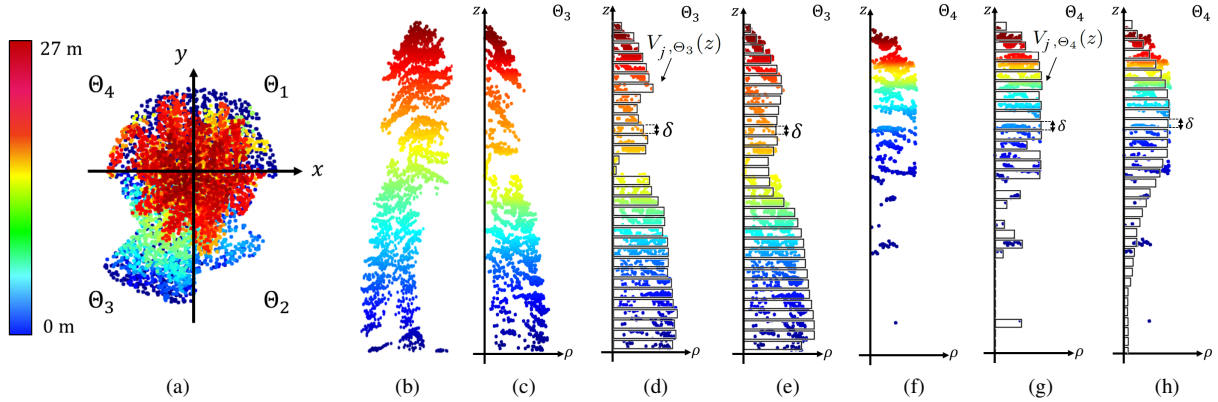

Fig. 3. Example of subdominant tree crown detection: (a) top view of the dominant tree crown $\mathcal{C}_k$ divided into L angular sectors, with L=4, (b) side view of the dominant tree crown, (c) vertical profile of the projected LiDAR points $\Pi_c(\mathbf{p}_i) \in \mathcal{C}_{k,\Theta_3}$, where the subdominant crown is present, (d) vertical profile quantization performed to obtain $V_{k,\Theta_3}(z)$, (e) $V_{k,\Theta_3}(z)$ after the Gaussian filtering, (f) vertical profile of the projected LiDAR points $\Pi_c(\mathbf{p}_i) \in \mathcal{C}_{k,\Theta_4}$, where no subdominant crowns are present, (g) vertical profile quantization performed to obtain $V_{k,\Theta_4}(z)$, (h) $V_{k,\Theta_4}(z)$ after the Gaussian filtering.

to smooth the profile and reduce the noise introduced by the tree branches (see Fig. 3e and Fig. 3h). It is worth noting that, unlike the 1D discrete signal $S_{k,\Theta_j}(\rho)$ generated to perform the derivative analysis, $V_{k,\Theta_j}(z)$ depends on the variable z (instead of ρ) since we are interested in the vertical profile of the tree rather than in the horizontal one. By computing the discrete derivative $V'_{k,\Theta_j}(z)$, we aim to the detect the presence of a local minimum which corresponds to the height of treetop of the subdominant crown $H^{\text{sub}}_{k,\Theta_j}$ located in the angular sector Θ_j, i.e.,:

$$H^{\text{sub}}_{k,\Theta_j} = V_{k,\Theta_j}(z_0), \text{ with } z_0 = \underset{z}{\text{argmin}}\{V_{k,\Theta_j}(z)\} \quad (4)$$

Thus, if a local minimum is detected, we assume the presence of a subdominant tree in $\mathcal{C}_{k,\Theta_j}$ (see Fig. 3e), whereas if no local minima are identified we assume there is no understory vegetation in $\mathcal{C}_{k,\Theta_j}$ (see Fig. 3h). Let us define with $\mathcal{C}^{\text{sub}}_{k,\Theta_j}$ the sectors where a subdominant crown has been identified. To detect the ground coordinates of the treetop $(x^{\text{sub}}_k, y^{\text{sub}}_k)$ we consider only the set of LiDAR points $\mathcal{P}^{\text{sub}}_{k,\Theta_j}$ defined as:

$$\mathcal{P}^{\text{sub}}_{k,\Theta_j} = \left\{ \mathrm{p}_i \in \mathcal{C}^{\text{sub}}_{k,\Theta_j} \middle| z_i \leq H^{\text{sub}}_{k,\Theta_j} \right\} \quad (5)$$

Therefore, we generate the raster image of $\mathcal{P}^{\text{sub}}_{k,\Theta_j}$ and we detect the treetop of the subdominant tree by applying the Level Set Method to the obtained CHM representing the understory vegetation (See Fig. 4). In particular, adjacent angular sectors are rasterized in the same image to assess if they represent the same subdominant tree or different ones. In contrast, nonadjacent angular sectors are rasterized separately. Indeed, unlike the methods presented in the literature [28], [29], [30], the angular analysis allows us to detect the presence of more than one subcanopy below the same dominant tree. Moreover, the circular projection emphasizes the presence of the subdominant crowns, thus facilitating the detection. At the end of this step, we obtain the set of treetops of the subdominant trees $\mathcal{T}_{\text{sub}} = \{\mathbf{t}^{\text{sub}}_1, \mathbf{t}^{\text{sub}}_2, .., \mathbf{t}^{\text{sub}}_G\}$, where around each treetop $\mathbf{t}^{\text{sub}}_k$ we have the LiDAR point sectors associated to $\mathbf{t}^{\text{sub}}_k$, i.e., $\mathcal{P}^{\text{sub}}_k = \{\mathcal{P}^{\text{sub}}_{k,\Theta_1}, .., \mathcal{P}^{\text{sub}}_{k,\Theta_S}\}$, with $S \leq L$.

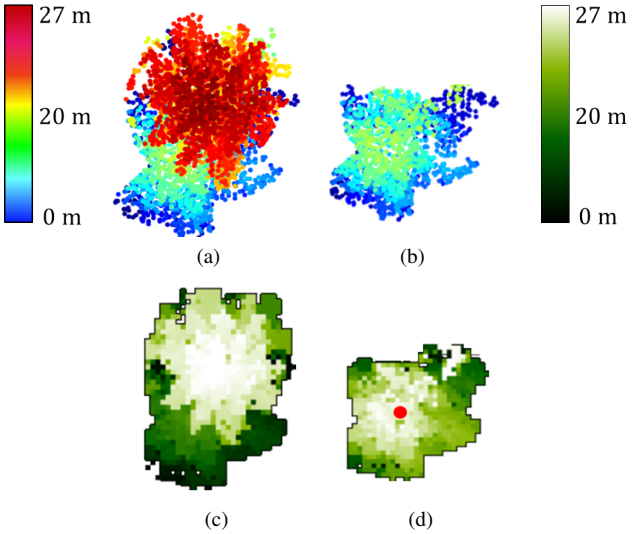

Fig. 4. Example of subdominant tree detection: (a) top view of the dominant tree crown $\mathcal{C}_k$ in the PCS, (b) top view of the subdominant tree in the PCS obtained keeping the set of LiDAR point $\mathcal{P}^{\text{sub}}_k = \{\mathcal{P}^{\text{sub}}_{k,\Theta_2}, \mathcal{P}^{\text{sub}}_{k,\Theta_3}\}$, (c) CHM of the dominant tree crown, (d) CHM of the subdominant tree crown, where the detected treetop is highlighted in red.

D. Crown Delineation of subdominant Trees

At the end of the detection step, we aim at extracting the crowns of all the detected subdominant trees. Thus, for each treetop $\mathbf{t}^{\text{sub}}_k$ we consider the associated LiDAR point cloud $\mathcal{P}^{\text{sub}}_k$. Then, as in the dominant layer of the forest, we apply the angular analysis to automatically delineate the crown boundaries of the trees belonging to the subdominant layer of the forest. In particular, for each treetop $\mathbf{t}^{\text{sub}}_k$ we extract the crown $\mathcal{C}^{\text{sub}}_k$, thus generating the set of subcanopies $\{\mathcal{C}^{\text{sub}}_1, \mathcal{C}^{\text{sub}}_2, .., \mathcal{C}^{\text{sub}}_G\}$.

III. Dataset Description

The proposed method was tested on two LiDAR datasets acquired in different geographical areas with different laser

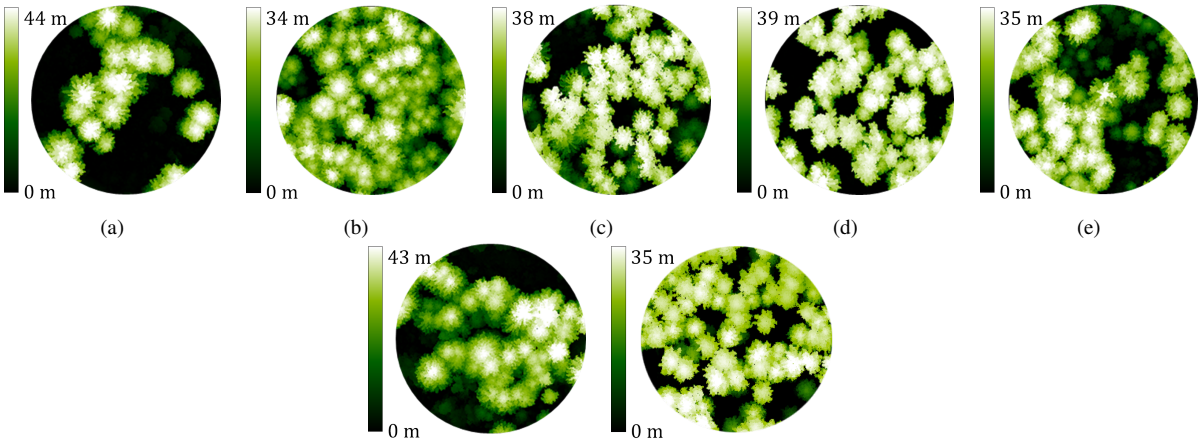

Fig. 5. False color representation of the raster images representing the investigated stand plots for the high-density LiDAR dataset (i.e., 15 pts/m^2). (a) Sample Plot H1, (b) Sample Plot H2, (c) Sample Plot H3, (d) Sample Plot H4, (e) Sample Plot H5, (f) Sample Plot H6, (g) Sample Plot H7. The rasterization has been performed with a spatial resolution of 25 cm.

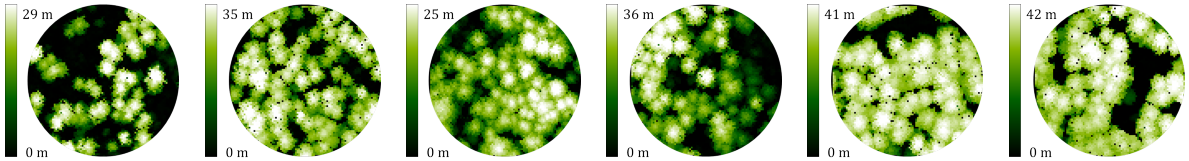

Fig. 6. False color representation of the raster images representing the investigated stand plots for the low-density LiDAR dataset (i.e., 5 pts/m^2). (a) Sample Plot L1, (b) Sample Plot L2, (c) Sample Plot L3, (d) Sample Plot L4, (e) Sample Plot L5, (f) Sample Plot L6. The rasterization has been performed with a spatial resolution of 50 cm.

TABLE I

NUMBER OF TREES, TREE HEIGHT (H) AND CROWN RADIUS (CR) PRESENTED DIVIDED PER STANDS PLOT FOR THE: (a) HIGH-DENSITY LIDAR DATA, (b) LOW-DENSITY LIDAR DATA. WHILE THE NUMBER AND THE HEIGHT OF THE TREES WERE MEASURED IN SITU, THE CROWN RADII WERE MANUALLY DELINEATED BY VISUAL INTERPRETATION.

Plot	Trees	H (m)		CR (m)	
		Range	Mean	Range	Mean
H1	14	34 - 44	38.4	2.9 - 5.5	4.4
H2	33	20.7 - 33.5	28.5	1.6 - 5.9	3.3
H3	37	24 - 37.4	33.2	2.1 - 4.1	3.1
H4	28	28.2 - 39.8	35.3	2.5 - 6.2	3.9
H5	31	3.6 - 35	23.6	1.2 - 5.2	2.8
H6	39	15 - 42.4	32.1	1.8 - 6.4	3.5
H7	36	27 - 35	31.3	1.6 - 4.5	3.1

(a)

Plot	Trees	H (m)		CR (m)	
		Range	Mean	Range	Mean
L1	33	4.4 - 28.3	21.4	1.1 - 3.6	2.3
L2	50	3.9 - 34.6	28.6	1.1 - 3.2	2.3
L3	24	16.6 - 24.4	20.6	1.3 - 3.6	2.4
L4	36	7.7 - 35.9	25	1.3 - 3.2	2.3
L5	45	34.6 - 40.5	38.1	2.1 - 3.2	4.1
L6	29	31.6 - 41.9	38.4	2.3 - 5.1	3.2

(b)

point density, hereafter referred to as the high-density (i.e., average point density of 15 pts/m^2) and the low-density dataset (i.e., average point density of 5 pts/m^2). Both the study areas are coniferous forests located in the Southern Italian Alps, a mountainous scenario characterized by a complex terrain's morphology (steep slopes and wide range of elevation).

The high-density LiDAR data were acquired in the municipality of Pellizzano, Trentino region. The coordinates of the central point of this area are $46°17'31{,}00''$ N, $10°45'56{,}49''$ E. The data were acquired between 7th and 9th of September 2012 with a Riegl LMS - Q680i sensor mounted on an airborne platform. The aircraft was flying at a speed of about 180 km/h at an altitude of approximately 660 m above the ground level. The pulse repetition frequency was 400 kHz. For each laser pulse four returns were recorded, with an average point density of 15 pts/m^2 (up to 50 pts/m^2). The area extends approximately 3200 Ha and the altitude ranges from 900 to 2000 meters a.s.l.. The species composition of the forest is mainly Norway Spruce and European Larch. Field data were collected in 7 circular sample plots having radius 20 m (see Fig. 5). The stands represent different forest structure in

terms of crown size and forest density. Moreover, all of them are uneven-aged forest (i.e., inside the stand plot the trees have three or more distinct age classes), thus representing a complex test case. Within each sample plot, the trees have been surveyed by recording the tree position (x, y coordinates), the tree height, the species, whereas we manually delineated the crown radius by means of an accurate visual interpretation (see Table Ia). To this end trees were displayed in the 3D LiDAR point cloud and the crown boundaries were manually drawn by an independent experienced operator. The crown segmentation was based on visual interpretation of the crown geometry both from the top and the side view of the considered tree. Because of the lack of subdominant trees in the sample plots, from the entire forest area a subset of 171 dominant trees were considered for validation purpose, 85 of which contain subdominant trees below, and 86 without subcanopies. The presence of both the dominant and the subdominant trees was checked individually in the PCS to generate the reference data. The crown radii of the subdominant trees were manually delineated by visual interpretation.

The low-density LiDAR data were acquired on 4th September 2007 at Parco Naturale Paneveggio - Pale di San Martino, by means of an Optech ALTM 3100EA sensor. The coordinates of the central point of this area are $46°17'47{,}60''$ N, $11°45'29{,}98''$ E. For each laser pulse four returns were recorded, with an average point density for the first return of at least 5 pts/m^2. The pulse wavelength and the pulse repetition frequency are 1064 nm and 100 kHz, respectively. The area extends for 368 Ha and the altitude ranges between 1536 m and 2065 m. The dominant species are Norway Spruce and Silver Fir. Ground data are available in 6 circular stands plot of radius 20 m (see Fig. 6). Within each stand plot, all the trees were measured. For each surveyed tree, the geographical position (measured with respect to the center of the sample plot), the tree height, the species and the projected crown area were recorded. The crown radii were manually delineated in the PCS for validation purpose (see Table Ib).

To link the field measured trees with the segmented crowns, the plot center coordinates were first manually corrected by matching the dominant trees positions measured in situ with the treetops visible in the CHM. In particular, each detected tree has been associated to a field measured tree considering a maximum horizontal distance d_{xy} of 2 m and a maximum height difference d_h of 3 m.

IV. Parameter Analysis and Experimental Setup

Tab. II presents the recommended values for the parameters of the proposed approach for the high- and the low-density LiDAR data. These values have been used in all the experiments presented in this paper. The tuning of the parameters was carried out by considering only the properties of the LiDAR point cloud without any prior knowledge on the average crown size and forest density. The spatial resolution of the CHM was selected on the basis of the average number of LiDAR pts/m^2, while the values of the 2D Gaussian filtering parameters were tuned in order to remove small variations on the crown surface. Thus, the degree of smoothness is based on the spatial resolution of the image to avoid commission errors. Accordingly, these values were the same for all the sample plots in the same dataset.

TABLE II
Recommended values for the parameters of the proposed approach for the high- and the low- density datasets. The choice of the values is based only on the properties of the LiDAR data.

	Parameters	Values	
		High-Density	**Low-Density**
Dominant	Spatial Resolution of the CHM	0.25 m	0.50 m
	2D Filter Kernel Size	5×5	3×3
	2D Filter Standard Deviation	10	5
	Search Radius R	20	20
	# of Angular Sectors N	8	8
	Horizontal Quantization Step ξ	0.30 m	0.60 m
	1D Filter Kernel Size	1×3	1×3
	1D Filter Standard Deviation	4	4
subdominant	# of Angular Sectors L	4	-
	# of Vertical Quantization Step D	29	-
	1D Filter Kernel Size	1×7	-
	1D Filter Standard Deviation	4	-

The angular analysis was performed by considering $N = 8$ sectors with $\Theta = 45°$, which turned out to be effective for both the treetop detection and the crown delineation in the PCS regardless of the laser sampling density. Note that the value $\Theta = 45°$ represents accurately the different sides of a crown. To quantize the distance between the LiDAR points and the treetop $\mathbf{t}_k$ in each angular sector, ξ should be tuned taking into account the LiDAR point density to guarantee at least one LiDAR point per interval. In the considered datasets, ξ was equal to 0.3 m and to 0.6 m for the high- and the low-density LiDAR datasets, respectively (note that we have at least 15 pts/m^2 in the first case and 5 pts/m^2 in the second case). The Gaussian filtering applied to the 1D discrete signal $S_{k,\Theta_j}(\rho)$ used for smoothing the crown profile and removing the outliers had a window size of 1×3, which can be used regardless of the LiDAR density and the crown size.

To perform the detection of the subdominant crowns the number of angular sectors was fixed to $L = 4$. Thus, the subdominant trees were analyzed in four different portions of the dominant tree crown. From our experiments it turned out that in each sector an average of 20 LiDAR points for each quantization step δ is required to properly represent $V_{k,\Theta_j}(z)$. In our dataset, this condition was achieved setting $D = 29$, thus adapting the size of δ to the height of the crown. Accordingly, we fixed this value to perform all the experiments presented in this paper. Fig. 7 shows the behaviour of the number of detected trees and true negatives versus the value of D. Note that the detection rate of subdominant trees increases as the value of D does. However, it leads to a lower detection of a true negative (i.e., high detection of false positive). Indeed, increasing the number of steps implies a better representation of the tree structure, but the number of LiDAR points per step δ decreases. Moreover, with too fine quantization scale some false trees can be detected because

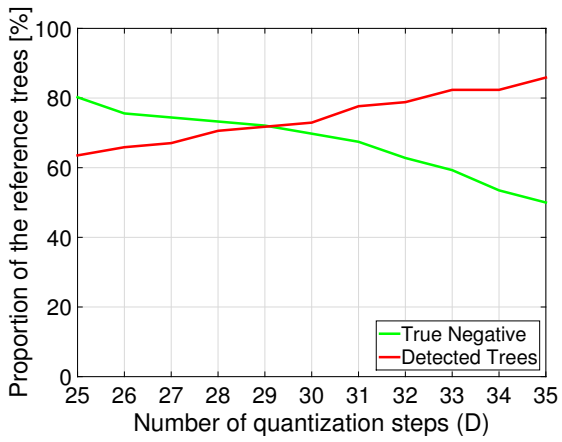

Fig. 7. Behaviour of the vertical quantization step D vs the number of detected trees and true negatives for the subdominant layer of the forest.

of the possible geometrical anomalies present in the vertical profile of the crown. Therefore, to obtain accurate detection results, it is necessary to have a reliable representation of the crown guaranteeing a minimum amount of LiDAR points per step.

For the detection of the dominant trees, the proposed method (PM) was compared with two standard state-of-the-art methods: i) the Level Set Method (LSM) [42], and ii) the Local Maxima Filtering (LMF) [4]. The in situ reference measures were used to assess the detection accuracy. In particular, the results were evaluated by considering the Detection (DET) Accuracy (number of trees associated to the field data), the Omission (OM) Error (number of missed trees) and the Commission (COM) Error (number of trees detected which are not associated to any field data). Both the state-of-the-art methods detect the trees only in the image domain. Therefore, the results are strongly affected by the degree of smoothing applied to the CHM. Moreover, while the LSM progressively slices the CHM to detect the treetop [42], the LMF exploits a sliding window to search the local peaks. Thus, the applied window size affects the detection results. Accordingly, a tuning of the state of the art algorithms on a training set was necessary to ensure the best performance per forest type.

To evaluate the performance of the proposed method on the subdominant layer of the forest, we considered the set of 171 trees selected in the high-density LiDAR data. No in situ measures were available for these trees, thus the presence of the both the dominant and the subdominant trees were checked manually in the PCS according to the procedure discussed in the previous section. In this case, the Detection (DET) Accuracy and the Omission (OM) Error represent the number of detected trees and the number of false negatives in proportion to the number of real subdominant trees (i.e., 85), respectively. The Commission (COM) Error represents the number of false positives in proportion to the number of dominant trees without subcanopies (i.e., 86). Finally, the Overall Accuracy (OA) metric evaluates both the correct identification of the presence or absence of the subdominant trees in proportions to the total amount of trees (i.e., 171). In this case the PM was compared with the Height Frequency Distribution method (HFD) presented in [28] and [29]. However, due to the assumption of double layer forest stands (not true for the considered dataset) in the latter case the technique resulted in both many commission errors and low detection rate. Thus, here we do not report the numerical results obtained. As we are interested in the comparison of the detection of the subdominant trees, we considered the same set of dominant tree crowns extracted in the previous step for both the HFD and the PM.

To quantitatively assess the crown delineation results the automatic segmentation results were compared with the crown radii identified by visual interpretation for both the dominant and the subdominant trees. The following empirical metrics were considered: the statistical determination coefficient ($R^2 \in [0, 1]$), the Mean Error (ME $\in [0, \infty]$), the Mean Absolute Error (MAE $\in [0, \infty]$), the Mean Square Error (MSE $\in [0, \infty]$) and the Normalized Mean Square Error (NRMSE $\in [0, \infty]$). Note that, the NRMSE is presented to facilitate the comparison between datasets due to the different crown radius (CR). Thus, it is computed as the ratio between the RMSE and the range of the measured CR (i.e., CR_{max} - CR_{min}).

V. Experimental Results and Discussion

A. Dominant Layer of the forest

Tab. IIIa and IIIb show the detection results obtained with the PM, the LSM and the LMF on the high- and the low-density datasets, respectively. Although the CHM provides the full representation of the dominant layer of the forest, the LSM and the LMF did not detect all the trees present in the scene due to the high canopy density. In particular, the LMF achieved a lower detection rate compared to the LSM because of the window size, which was tuned to fit the larger crowns (to avoid too many false tree detections), thus penalizing the detection of the smaller crowns. This condition has less of an effect on the detection results for the low-density dataset (i.e., 183 trees detected compared to the 184 identified with the LSM) since the forest stands are characterized by homogeneous crown size (see Fig. 6). In contrast, the choice of the window size strongly affects the detection in the high-density dataset characterized by uneven-aged stands (i.e., 194 trees detected compared to the 204 identified with the LSM).

Differently from the state-of-the-art methods, the proposed approach exploits the information provided by the original LiDAR point cloud to refine the detection performance achieved in the CHM. Indeed, the detection results obtained in the CHM are affected by the interpolation process and the smoothing filtering, whereas in the PCS the convex shape of the tree crowns is clearly visible. Moreover, the proposed approach is capable of handling the crown size variability within the same forest stand since it relies on the geometrical properties of the tree crowns. Thus, due to the further analysis in the PCS, the proposed method improved the detection rate regardless of the laser point density. This was achieved by keeping the commission errors under 7% and 2% for the high- and the low- density dataset, respectively. In particular, in the high-density dataset the PM identified 8 and 18 trees more than the

TABLE III
TREE DETECTION RESULTS FOR THE DOMINANT LAYER OF THE FOREST OBTAINED ON: (a) THE HIGH-DENSITY LIDAR DATASET, (b) THE LOW-DENSITY LIDAR DATASET. THE DETECTION ACCURACY (DET), COMMISSION (COM) AND OMISSION (OM) ERRORS ARE PRESENTED DIVIDED PER STAND PLOT. THE PROPOSED METHOD (PM) IS COMPARED WITH THE STANDARD LEVEL SET METHOD (LSM) AND LOCAL MAXIMA FILTERING (LMF).

		Proposed Method (PM)			**Level Set Method (LSM)**			**Local Maxima Filtering (LMF)**		
Plot	**# Trees**	**DET**	**COM**	**OM**	**DET**	**COM**	**OM**	**DET**	**COM**	**OM**
H1	14	13 (92.8%)	2 (14.3%)	1 (7.1%)	13 (92.8%)	2 (14.3%)	1 (7.1%)	11 (78.6%)	3 (21.4%)	3 (21.4%)
H2	33	30 (90.9%)	0 (0%)	3 (9.1%)	28 (84.8%)	0 (0%)	5 (15.2%)	26 (78.8%)	0 (0%)	7 (21.2%)
H3	37	36 (97.3%)	4 (10.8%)	1 (2.7%)	31 (83.8%)	4 (10.8%)	6 (16.2%)	31 (83.8%)	2 (5.4%)	6 (16.2%)
H4	28	28 (100%)	4 (14.3%)	0 (0%)	28 (100%)	2 (7.1%)	0 (0%)	27 (96.4%)	0 (0%)	1 (3.6%)
H5	31	31 (100%)	1 (3.2%)	0 (0%)	31 (100%)	0 (0%)	0 (0%)	28 (90.3%)	3 (9.7%)	3 (9.7%)
H6	39	38 (97.4%)	1 (2.6%)	1 (2.6%)	38 (97.4%)	1 (2.6%)	1 (2.6%)	36 (92.3%)	0 (0%)	3 (7.7%)
H7	36	36 (100%)	2 (5.6%)	0 (0%)	35 (97.2%)	2 (5.6%)	1 (2.8%)	35 (97.2%)	2 (5.6%)	1 (2.8%)
Total	218	212 (97.2%)	14 (6.4%)	6 (2.8%)	204 (93.6%)	11 (5%)	14 (6.4%)	194 (89.0%)	10 (4.6%)	24 (11%)

(a)

		Proposed Method (PM)			**Level Set Method (LSM)**			**Local Maxima Filtering (LMF)**		
Plot	**# Trees**	**DET**	**COM**	**OM**	**DET**	**COM**	**OM**	**DET**	**COM**	**OM**
L1	33	31 (93.9%)	0 (0%)	2 (6.1%)	28 (84.8%)	0 (0%)	5 (15.2%)	26 (78.8%)	0 (0%)	7 (21.2%)
L2	50	46 (92%)	0 (0%)	4 (8%)	41 (82%)	0 (0%)	9 (18%)	43 (86%)	0 (0%)	7 (14%)
L3	24	22 (91.7%)	1 (4.2%)	2 (8.3%)	20 (83.3%)	0 (0%)	4 (16.7%)	20 (83.3%)	0 (0%)	4 (16.7%)
L4	36	34 (94.4%)	0 (0%)	2 (5.6%)	31 (86.1%)	0 (0%)	5 (13.9%)	29 (80.6%)	0 (0%)	7 (19.4%)
L5	45	41 (91.1%)	1 (2.2%)	4 (8.9%)	40 (88.9%)	0 (0%)	5 (11.1%)	38 (84.4%)	0 (0%)	7 (15.6%)
L6	29	26 (89.7%)	1 (3.4%)	3 (10.3%)	24 (82.8%)	0 (0%)	5 (17.2%)	27 (93.1%)	0 (0%)	2 (6.9%)
Total	217	200 (92.2%)	3 (1.4%)	17 (7.8%)	184 (84.8%)	0 (0%)	33 (15.2%)	183 (84.3%)	0 (0%)	34 (15.7%)

(b)

LSM and the LMF, respectively, whereas it introduced only 3 and 4 commission errors more than the LSM and the LMF, respectively. In the low-density dataset the PM identified 16 trees more than the LSM and 17 more than the LMF, while incurring only 3 additional commission errors.

Note that on the high-density dataset we obtained higher detection rate (i.e., 97.2%) than in the low-density dataset (i.e., 92.2%) because of the better characterization of the 3D structure of the forest. However, while in the high-density case the CHM provided enough information to detect the majority of the trees (the spatial resolution of the CHM is 0.25 m), in the low-density case the analysis of the PCS allowed us to halve the omission errors obtained with the LSM (i.e., from 33 to 17 missed trees). This reduction of the omissions strongly improves the estimation of forest parameters such as volume and structure, especially when dealing with trees characterized by an average height that ranges from 23.6 m to 38.4 m in Pellizzano (see Tab. Ia) and from 20.6 m to 38.4 m in Paneveggio (see Tab. Ib).

Let us now address the crown delineation results. Fig. 8a and Fig. 8b show the scatterplots of the real versus the estimated crown radius of the correctly detected trees for the high- and the low- dataset, respectively. The scatterplots show the capability of the angular analysis to properly delineate the single tree crowns regardless of the forest density and the laser sampling density. As expected, the high-density dataset resulted in a better delineation of the crown edges. However, the error metrics point out that we obtained accurate results in both of the datasets. Indeed, R^2 ranges between 0.78 to 0.82, whereas the NRMSE ranges from 7.96% and 8.75%. Due to the missed detection of some trees, we have some cases of over-segmented crowns. For a complete evaluation of the method Tab. IV presents the error metrics of the estimated crown radius divided per dataset. By taking into account all the sources of errors, we obtained a MAE of 0.52 m, on an average crown radius of 3.4 m, for the high-density dataset (i.e., 15.3%), and a MAE of 0.51 m on an average crown radius of 2.6 m, for the low-density dataset (i.e., 19.6%). A qualitative evaluation of the segmentation results confirms the effectiveness of the angular analysis in detecting the crown boundaries. Fig. 9 shows some examples of crown delineation results by presenting the segmented trees in the forest area for the high-density (Fig. 9a - Fig.9f) and the low-density LiDAR dataset (Fig. 9g - Fig. 9l). As one can notice, the segmentation method was able to delineate the crowns of detected trees, despite the presence of overlapping and asymmetric crowns.

B. Subdominant Layer of the forest

Tab. V presents the values of the quality metrics obtained by the PM and the HFD [28] in the detection of the subdominant trees. As one can notice, both methods achieve similar performances in terms of number of detected trees (i.e., 61 with the

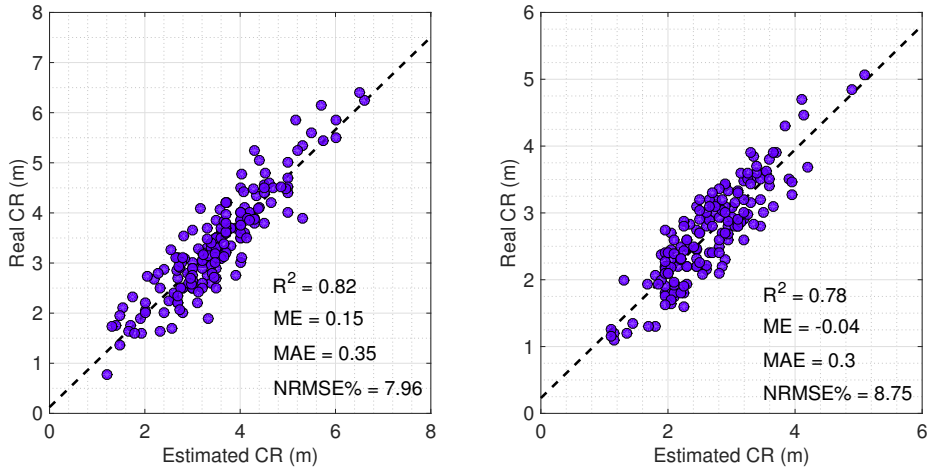

(a) (b)

Fig. 8. Real versus estimated (with the proposed method) crown radius (CR) of the dominant trees for: (a) the high-density LiDAR dataset, (b) the low-density LiDAR dataset.

TABLE IV
ME, MAE, MSE AND NRMSE OF THE ESTIMATED CROWN RADIUS ARE PRESENTED DIVIDED PER DATASET. THE ERROR METRICS INCLUDE THE OVER-SEGMENTATION ERROR DUE TO THE OMISSION ERRORS.

Dataset	ME	MAE	MSE	NRMSE
High-density	0.38 m	0.52 m	0.81	16.8%
Low-density	-0.26 m	0.51 m	0.59	15.1%

TABLE V
DETECTION ACCURACY (DET), COMMISSION ERRORS (COM), OMISSION ERRORS (OM) AND OVERALL ACCURACY (OA) OBTAINED FOR THE SUBDOMINANT LAYER OF THE FOREST WITH THE PROPOSED METHOD (PM) AND THE REFERENCE METHOD (HFD).

	DET	COM	OM	OA
PM	61 (71.8%)	24 (27.9%)	24 (28.3%)	123 (71.9%)
HFD	66 (77.6%)	43 (50%)	19 (22.3%)	109 (63.7%)

PM and 66 with the HFD), whereas the proposed approach strongly reduced the number of false trees detected (i.e., 24 compared to 43). Note that, while the proposed method analyzes the geometrical structure of the vertical profile, the HFD detects the anomalies in the vertical profile of the crown (i.e., the presence of understory vegetation) considering the frequency height distribution. However, when dealing with dense forest scenarios the trees are very close to each other and thus, the shape of the dominant crowns is not symmetric. Accordingly, the presence of anomalies in the frequency height distribution is poorly correlated to the presence of understory vegetation as proved by the commission errors. In contrast, the angular analysis allows us to address the issue of anisotropic crowns. Moreover, the projection of the laser points onto the ρz plane (accomplished to represent the vertical profile of the tree) further reduces the influence of the asymmetry of the crown in the detection of the subdominant trees. Thus, the overall accuracy is improved due to both the angular analysis which allows the detection of subdominant trees present in different portions of the crown and the circular projection step which emphasizes the presence of the subdominant crowns. The quantitative evaluation presented in Fig. 10 confirms the accuracy of the proposed approach in delineating the sub-canopies. Fig. 11 shows a qualitative example of the segmentation results obtained for the subdominant trees. A visual analysis confirms the effectiveness of the segmentation method in extracting the shape of the crown. Due to the angular analysis, the small trees can be extracted even though they are really close to the trunk of the dominant tree crown.

VI. CONCLUSION

In this paper a hierarchical approach to the 3D segmentation of LiDAR data at single-tree level in multilayered forest has been proposed. The proposed method: i) detects the dominant trees by exploiting both the image (CHM) and the LiDAR point cloud (PCS) to identify all the trees present in the scene, ii) delineates the dominant tree crowns in the PCS by exploiting the conical shape properties of the crown, iii) detects the subdominant trees by a derivative analysis of the 3D vertical profile of the dominant tree crowns, and iv) delineates the understory vegetation by applying a segmentation algorithm directly in the PCS domain.

From the analysis of the experimental results we can draw the following conclusions. The proposed approach improves the detection rate of the dominant tree crowns with respect to the standard methods at the state-of-the-art. This is accomplished by refining the detection achieved in the CHM considering the information provided by the original LiDAR point cloud, which is not affected by the interpolation process and the smoothing filtering. It is worth mentioning that the detection improvement is achieved by keeping the commission error rate under 7% for both datasets. Moreover, the detection

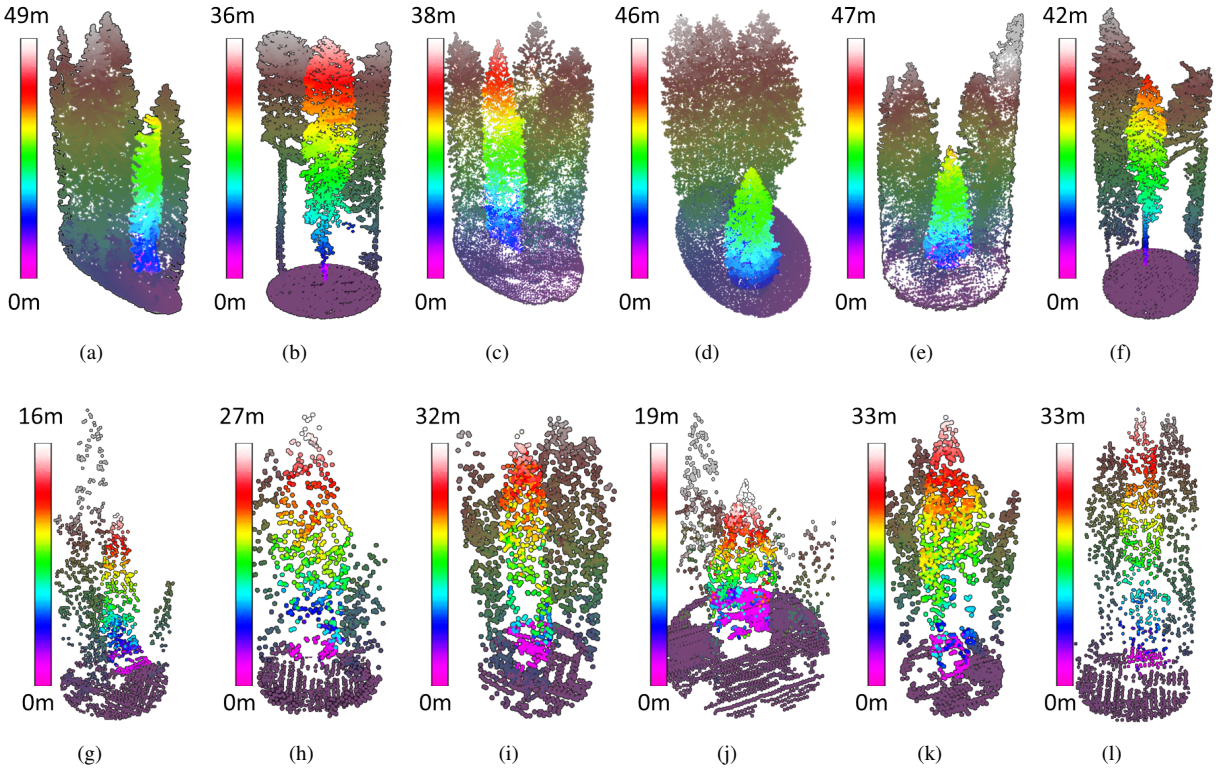

Fig. 9. Qualitative example of tree crown segmentation obtained in the dominant layer of the forest for: (a)-(f) the high-density LiDAR data and, (g)-(l) the low-density LiDAR data. The segmented crowns (represented in bright colors) are located in the original forest scenario. A visual analysis confirms that the proposed method is able to properly extract trees both in dense canopy scenario and when they are isolated regardless of the laser point density.

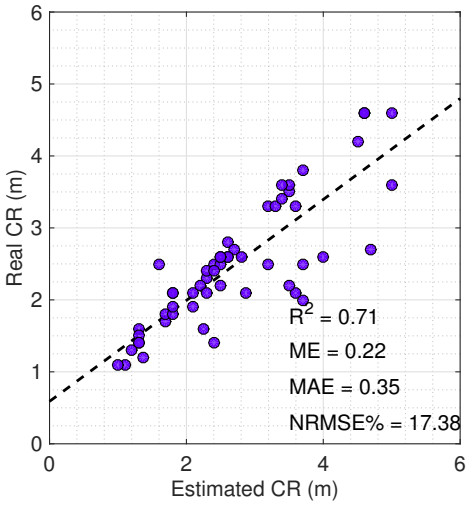

Fig. 10. Real versus estimated (with the proposed method) crown radius (CR) of the subdominant trees.

performed in the PCS proved to be robust with respect to the forest density and the average crown size since it relies on the geometrical properties of the tree crowns, thus addressing the issue of segmenting heterogeneous forest stands (i.e., high crown size variability). Indeed, results on the high-density dataset demonstrate that the method can be applied to heterogeneous forests by using the same set of parameters. Note that, the tuning of parameters was accomplished by considering only the properties of the LiDAR data without using any prior knowledge or training procedure. Finally, the angular analysis of the vertical profile of the crown of the proposed method drastically reduced the commission errors in the detection of trees in the subdominant layer of the forest. Furthermore, the proposed method also detected multiple trees present below the dominant crowns. Also in this case, the detection rate was better than the one obtained with the method presented in the literature.

As a final remark, we can conclude that the proposed segmentation method is able to fit the shape of the trees for both the dominant and the subdominant layers of the forest. Indeed, the angular analysis performed in the PCS is able to adapt the crown delineation different portion separately.

As future developments of this work, we aim at testing the proposed method on LiDAR data characterized by different point densities and in forests having properties different from the one used in the paper. Moreover, we plan to test the effectiveness of the proposed approach on the full waveform LiDAR data.

VII. Acknowledgement

The authors would like to thank the “Dipartimento Risorse Forestali e Montane” of the Autonomous Province of Trento for providing the high- density and low-density LiDAR data used in this study in the framework of the FORLIDAR project.

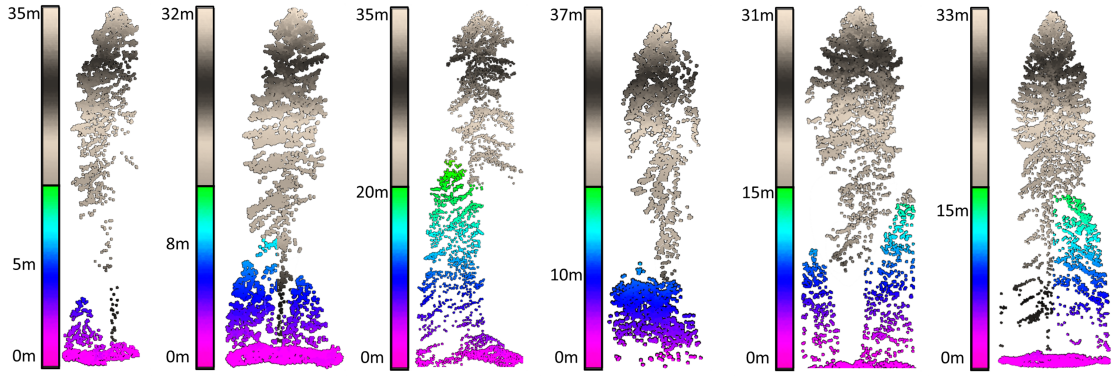

(a) (b) (c) (d) (e) (f)

Fig. 11. Qualitative example of tree crown segmentation obtained in the subdominant layer of the forest (high-density LiDAR dataset). (a)-(f) the segmented crowns are represented in bright colors in the original forest scenario.

APPENDIX

The mathematical notation used in this paper is listed in Tab. VI. Symbols are listed in the order of appearance.

TABLE VI
NOTATION USED IN THIS PAPER.

Symbol	**Description**
$\mathcal{P} = \{\mathbf{p}_i\}_{i=1}^{A}$	Set of LiDAR points of the PCS, with $\mathbf{p}_i = (x_i, y_i, z_i)$
$\mathcal{T}_{\text{CHM}} = \{\mathbf{t}_k\}_{k=1}^{M}$	Set of dominant treetops detected in the CHM, with $\mathbf{t}_k = (x_k^t, y_k^t, z_k^t)$
R	Given search radius
$\mathcal{P}_k$	Set of LiDAR points extracted around the treetop $\mathbf{t}_k$ within the given search radius R
N	Number of angular sectors used for the derivative analysis of the horizontal profile of the crowns
Θ_j	Angular sector between the adjacent angles θ_j and θ_{j+1}, with $j \in [0, N\text{-}1]$
$\mathcal{P}_{k,\Theta_j}$	Set of LiDAR points belonging to the angular sector Θ_j
Π_c	Circular projection that maps the LiDAR points into the ρz plane
ξ	Quantization step of the distance of the points from the treetop, $\rho_i \in [0, R]$
$S_{k,\Theta_j}(\rho)$	1-D discrete signal representing $\Pi_c(\mathcal{P}_{k,\Theta_j})$, where $\mathbf{p}_i = (\rho_i, z_i)$
M_{k,Θ_j}	Closest height maximum to the treetop $\mathbf{t}_k$, detected along ρ in the angular sector Θ_j
$\mathcal{T}_{\text{PCS}}$	Set of dominant treetop detected in the PCS
$\mathcal{T} = \{\mathbf{t}_k\}_{k=1}^{W}$	Whole set of detected treetop
E_{k,Θ_j}	Edge position of the kth tree detected in the angular sector Θ_j
$\{\mathcal{C}_k\}_{k=1}^{W}$	Set of dominant segmented tree crowns, with $\mathcal{C}_k = \{\mathbf{p}_1, .., \mathbf{p}_B\}$
L	Number of angular sectors used for the detection of the subdominant trees, with $L \leq N$
$\mathcal{C}_{k,\Theta_j}$	Set of LiDAR points of the crown $\mathcal{C}_k$ belonging to the angular sector Θ_j
$V_{k,\Theta_j}(z)$	1-D vertical signal representing $\Pi_c(\mathcal{C}_{k,\Theta_j})$, where $\mathbf{p}_i = (z_i, \rho_i)$
H_{k,Θ_j}	Maximum height value of the set of points $\mathcal{C}_{k,\Theta_j}$
δ	Quantization step of the vertical profile of dominant tree
$H_{k,\Theta_j}^{\text{sub}}$	Height of the subdominant tree detected in the angular sector Θ_j
$\mathcal{C}_k^{\text{sub},\Theta_j}$	LiDAR point sectors of the kth dominant crown where the subdominant crown has been detected
$\mathcal{P}_{k,\Theta_j}^{\text{sub}}$	Set of LiDAR points $\mathbf{p}_i \in \mathcal{C}_{k,\Theta_j}^{sub}$ having $z_i \leq H_{k,\Theta_j}^{\text{sub}}$
$\mathcal{T}_{\text{sub}} = \{\mathbf{t}_k^{\text{sub}}\}_{k=1}^{G}$	Set of treetops of the subdominant trees
$\{\mathcal{C}_k^{\text{sub}}\}_{k=1}^{G}$	Set of dominant segmented tree crowns.

REFERENCES

[1] T. Brandtberg, T. A. Warner, R. E. Landenberger, and J. B. McGraw, "Detection and analysis of individual leaf-off tree crowns in small footprint, high sampling density lidar data from the eastern deciduous forest in north america," *Remote sensing of Environment*, vol. 85, no. 3, pp. 290–303, 2003.

[2] M. Maltamo, K. Mustonen, J. Hyyppä, J. Pitkänen, and X. Yu, "The accuracy of estimating individual tree variables with airborne laser scanning in a boreal nature reserve," *Canadian Journal of Forest Research*, vol. 34, no. 9, pp. 1791–1801, 2004.

[3] S. C. Popescu, R. H. Wynne, and R. F. Nelson, "Measuring individual tree crown diameter with lidar and assessing its influence on estimating forest volume and biomass," *Canadian journal of remote sensing*, vol. 29, no. 5, pp. 564–577, 2003.

[4] J. Hyyppä, O. Kelle, M. Lehikoinen, and M. Inkinen, "A segmentation-based method to retrieve stem volume estimates from 3-d tree height models produced by laser scanners," *Geoscience and Remote Sensing, IEEE Transactions on*, vol. 39, no. 5, pp. 969–975, May 2001.

[5] J. Hyyppä, M. Schardt, H. Haggrén, B. Koch, U. Lohr, R. Paananen, H. Scherrer, H. Luukkonen, M. Ziegler, H. Hyyppä *et al.*, "High-scan: The first european-wide attempt to derive single-tree information from laserscanner data," *The Photogrammetric Journal of Finland*, 2001.

[6] K. Barbara, H. Ursula, and W. Holger, "Detection of individual tree crowns in airborne lidar data," *Photogrammetric Engineering and Remote Sensing*, vol. 72, no. 4, pp. 357–363, 2006.

[7] T. Hengl, "Finding the right pixel size," *Computers and Geosciences*, vol. 32, no. 9, pp. 1283 – 1298, 2006.

[8] L. Ene, E. Næsset, and T. Gobakken, "Single tree detection in heterogeneous boreal forests using airborne laser scanning and area-based stem number estimates," *International journal of remote sensing*, vol. 33, no. 16, pp. 5171–5193, 2012.

[9] S. Solberg, E. Næsset, and O. Bollandsas, "Single-tree segmentation using airborne laser scanner data in a structurally heterogeneous spruce forest," *Photogrammetric Engineering and Remote Sensing*, vol. 72, pp. 1369–1378, 2006.

[10] D. Tiede, G. Hochleitner, and T. Blaschke, "A full gis-based workflow for tree identification and tree crown delineation using laser scanning," in *ISPRS Workshop CMRT*, vol. 5, 2005, pp. 29–30.

[11] D.-A. Kwak, W.-K. Lee, J.-H. Lee, G. S. Biging, and P. Gong, "Detection of individual trees and estimation of tree height using lidar data," *Journal of Forest Research*, vol. 12, no. 6, pp. 425–434, 2007.

[12] U. Pyysalo and H. Hyyppä, "Reconstructing tree crowns from laser scanner data for feature extraction," *International Archives Of Photogrammetry Remote Sensing And Spatial Information Sciences*, vol. 34, no. 3/B, pp. 218–221, 2002.

[13] X. Yu, J. Hyyppä, M. Vastaranta, M. Holopainen, and R. Viitala, "Predicting individual tree attributes from airborne laser point clouds based on the random forests technique," {*ISPRS*} *Journal of Photogrammetry and Remote Sensing*, vol. 66, no. 1, pp. 28 – 37, 2011.

[14] J. N. Heinzel, H. Weinacker, and B. Koch, "Prior-knowledge-based single-tree extraction," *International journal of remote sensing*, vol. 32, no. 17, pp. 4999–5020, 2011.

[15] A. Persson, J. Holmgren, and U. Söderman, "Detecting and measuring individual trees using an airborne laser scanner," *Photogrammetric Engineering and Remote Sensing*, vol. 68, no. 9, pp. 925–932, 2002.

[16] J. Holmgren, A. Barth, H. Larsson, and H. Olsson, "Prediction of stem attributes by combining airborne laser scanning and measurements from harvesters," *Silva Fenn*, vol. 46, no. 2, pp. 227–239, 2012.

[17] T. Lahivaara, A. Seppanen, J. P. Kaipio, J. Vauhkonen, L. Korhonen, T. Tokola, and M. Maltamo, "Bayesian approach to tree detection based on airborne laser scanning data," *Geoscience and Remote Sensing, IEEE Transactions on*, vol. 52, no. 5, pp. 2690–2699, 2014.

[18] M. Vastaranta, M. Holopainen, X. Yu, J. Hyyppä, A. Mkinen, J. Rasinmki, T. Melkas, H. Kaartinen, and H. Hyyppä, "Effects of individual tree detection error sources on forest management planning calculations," *Remote Sensing*, vol. 3, no. 8, pp. 1614–1626, 2011. [Online]. Available: http://www.mdpi.com/2072-4292/3/8/1614

[19] L. Wallace, A. Lucieer, and C. S. Watson, "Evaluating tree detection and segmentation routines on very high resolution uav lidar data," *Geoscience and Remote Sensing, IEEE Transactions on*, 2014.

[20] S. Gupta, H. Weinacker, and B. Koch, "Comparative analysis of clustering-based approaches for 3-d single tree detection using airborne fullwave lidar data," *Remote Sensing*, vol. 2, no. 4, pp. 968–989, 2010.

[21] F. Morsdorf, E. Meier, B. Kötz, K. I. Itten, M. Dobbertin, and B. Allgöwer, "Lidar-based geometric reconstruction of boreal type forest stands at single tree level for forest and wildland fire management," *Remote Sensing of Environment*, vol. 92, no. 3, pp. 353–362, 2004.

[22] H. Lee, K. C. Slatton, B. Roth, and W. Cropper Jr, "Adaptive clustering of airborne lidar data to segment individual tree crowns in managed pine forests," *International Journal of Remote Sensing*, vol. 31, no. 1, pp. 117–139, 2010.

[23] M. Maltamo, K. Eerikäinen, J. Pitkänen, J. Hyyppä, and M. Vehmas, "Estimation of timber volume and stem density based on scanning laser altimetry and expected tree size distribution functions," *Remote Sensing of Environment*, vol. 90, no. 3, pp. 319 – 330, 2004.

[24] D. Riano, E. Meier, B. Allgöwer, E. Chuvieco, and S. L. Ustin, "Modeling airborne laser scanning data for the spatial generation of critical forest parameters in fire behavior modeling," *Remote Sensing of Environment*, vol. 86, no. 2, pp. 177–186, 2003.

[25] J. Reitberger, C. Schnörr, P. Krzystek, and U. Stilla, "3d segmentation of single trees exploiting full waveform lidar data," *ISPRS Journal of Photogrammetry and Remote Sensing*, vol. 64, no. 6, pp. 561–574, 2009.

[26] J. Shi and J. Malik, "Normalized cuts and image segmentation," *Pattern Analysis and Machine Intelligence, IEEE Transactions on*, vol. 22, no. 8, pp. 888–905, 2000.

[27] E. Lindberg, L. Eysn, M. Hollaus, J. Holmgren, and N. Pfeifer, "Delineation of tree crowns and tree species classification from full-waveform airborne laser scanning data using 3-d ellipsoidal clustering," *Selected Topics in Applied Earth Observations and Remote Sensing, IEEE Journal of*, vol. 7, no. 7, pp. 3174–3181, July 2014.

[28] A. Barilotti, F. Sepic, E. Abramo, and F. Crosilla, "Assessing the 3d structure of the single crowns in mixed alpine forests," *International Archives of Photogrammetry, Remote Sensing and Spatial Information Sciences*, vol. 36, no. 3/W49A, 2007.

[29] Y. Wang, H. Weinacker, and B. Koch, "A lidar point cloud based procedure for vertical canopy structure analysis and 3d single tree modelling in forest," *Sensors*, vol. 8, no. 6, pp. 3938–3951, 2008.

[30] L. Duncanson, B. Cook, G. Hurtt, and R. Dubayah, "An efficient, multi-layered crown delineation algorithm for mapping individual tree structure across multiple ecosystems," *Remote Sensing of Environment*, vol. 154, pp. 378–386, 2014.

[31] J. J. Richardson and L. M. Moskal, "Strengths and limitations of assessing forest density and spatial configuration with aerial lidar," *Remote Sensing of Environment*, vol. 115, no. 10, pp. 2640–2651, 2011.

[32] A. Ferraz, F. Bretar, S. Jacquemoud, G. Gonçalves, L. Pereira, M. Tomé, and P. Soares, "3-d mapping of a multi-layered mediterranean forest using als data," *Remote Sensing of Environment*, vol. 121, pp. 210–223, 2012.

[33] J. Lopatin, M. Galleguillos, F. E. Fassnacht, A. Ceballos, and J. Hernandez, "Using a multistructural object-based lidar approach to estimate vascular plant richness in mediterranean forests with complex structure," *Geoscience and Remote Sensing, IEEE Transactions on*, 2015.

[34] M. Maltamo, P. Packaln, X. Yu, K. Eerikinen, J. Hyyppä, and J. Pitknen, "Identifying and quantifying structural characteristics of heterogeneous boreal forests using laser scanner data," *Forest Ecology and Management*, vol. 216, no. 13, pp. 41 – 50, 2005.

[35] M. K. Jakubowski, Q. Guo, and M. Kelly, "Tradeoffs between lidar pulse density and forest measurement accuracy," *Remote Sensing of Environment*, vol. 130, pp. 245–253, 2013.

[36] J. Vauhkonen, L. Ene, S. Gupta, J. Heinzel, J. Holmgren, J. Pitkänen, S. Solberg, Y. Wang, H. Weinacker, K. M. Hauglin *et al.*, "Comparative testing of single-tree detection algorithms under different types of forest," *Forestry*, p. cpr051, 2011.

[37] J. Pitkänen, M. Maltamo, J. Hyyppä, and X. Yu, "Adaptive methods for individual tree detection on airborne laser based canopy height model," *International Archives of Photogrammetry, Remote Sensing and Spatial Information Sciences*, vol. 36, no. 8, pp. 187–191, 2004.

[38] T. L. Swetnam and D. A. Falk, "Application of metabolic scaling theory to reduce error in local maxima tree segmentation from aerial lidar," *Forest Ecology and Management*, vol. 323, pp. 158–167, 2014.

[39] R. Palenichka, F. Doyon, A. Lakhssassi, and M. B. Zaremba, "Multi-scale segmentation of forest areas and tree detection in lidar images by the attentive vision method," *Selected Topics in Applied Earth Observations and Remote Sensing, IEEE Journal of*, vol. 6, no. 3, pp. 1313–1323, 2013.

[40] C. Alexander, "Delineating tree crowns from airborne laser scanning point cloud data using delaunay triangulation," *International Journal of Remote Sensing*, vol. 30, no. 14, pp. 3843–3848, 2009.

[41] W. Li, Q. Guo, M. Jakubowski, and M. Kelly, "A new method for segmenting individual trees from the lidar point cloud." *Photogrammetric Engineering and Remote Sensing*, vol. 78, pp. 75–84, 2012.

[42] A. Kato, L. M. Moskal, P. Schiess, M. E. Swanson, D. Calhoun, and W. Stuetzle, "Capturing tree crown formation through implicit surface reconstruction using airborne lidar data," *Remote Sensing of Environment*, vol. 113, no. 6, pp. 1148 – 1162, 2009.

[43] S. Kim, R. J. McGaughey, H.-E. Andersen, and G. Schreuder, "Tree species differentiation using intensity data derived from leaf-on and leaf-off airborne laser scanner data," *Remote Sensing of Environment*, vol. 113, no. 8, pp. 1575–1586, 2009.

[44] B. Hu, J. Li, L. Jing, and A. Judah, "Improving the efficiency and accuracy of individual tree crown delineation from high-density lidar data," *International Journal of Applied Earth Observation and Geoinformation*, vol. 26, pp. 145–155, 2014.